The Msx1 Homeoprotein Recruits Polycomb to the Nuclear Periphery during Development

Citation: Wang, Jingqiang, Roshan M. Kumar, Vanessa J. Biggs, Hansol Lee, Yun Chen, Michael H. Kagey, Richard A. Young, and Cory Abate-Shen. "The Msx1 Homeoprotein Recruits Polycomb to the Nuclear Periphery During Development." Developmental Cell 21, no. 3 (September 2011): 575–588. © 2011 Elsevier Inc.

As Published: http://dx.doi.org/10.1016/j.devcel.2011.07.003

Publisher: Elsevier

Persistent URL: http://hdl.handle.net/1721.1/92052

Version: Final published version: final published article, as it appeared in a journal, conference proceedings, or other formally published context

Developmental Cell
Article

The Msx1 Homeoprotein Recruits Polycomb to the Nuclear Periphery during Development

Jingqiang Wang,[1,5] Roshan M. Kumar,[2,5,7] Vanessa J. Biggs,[1] Hansol Lee,[3,6] Yun Chen,[3,8] Michael H. Kagey,[2] Richard A. Young,[2,4,*] and Cory Abate-Shen[1,3,*]

[1]Departments of Urology and Pathology and Cell Biology, Herbert Irving Comprehensive Cancer Center, Columbia University, College of Physicians and Surgeons, New York, NY 10032, USA
[2]Whitehead Institute for Biomedical Research, Cambridge, MA 02142, USA
[3]Center for Advanced Biotechnology and Medicine, UMDNJ-Robert Wood Johnson Medical School, Piscataway, NJ 08854, USA
[4]Department of Biology, Massachusetts Institute of Technology, Cambridge, MA 02139, USA
[5]These authors contributed equally to this work
[6]Present address: Department of Biological Sciences, College of Natural Science, Inha University, 253 Yonghyun-dong, Nam-Gu, Incheon 402-751, Korea
[7]Present address: Department of Biomedical Engineering and Center for BioDynamics, Boston University, Boston, MA 02215, USA and Wyss Institute for Biologically Inspired Engineering, Harvard University, Boston, MA 02115, USA
[8]Present address: Center for Pharmacogenomics, Washington University in St. Louis, St. Louis, MO 63110, USA
*Correspondence: young@wi.mit.edu (R.A.Y.), cabateshen@columbia.edu (C.A.-S.)
DOI 10.1016/j.devcel.2011.07.003

SUMMARY

Control of gene expression during development requires the concerted action of sequence-specific transcriptional regulators and epigenetic modifiers, which are spatially coordinated within the nucleus through mechanisms that are poorly understood. Here we show that transcriptional repression by the Msx1 homeoprotein in myoblast cells requires the recruitment of Polycomb to target genes located at the nuclear periphery. Target genes repressed by Msx1 display an Msx1-dependent enrichment of Polycomb-directed trimethylation of lysine 27 on histone H3 (H3K27me3). Association of Msx1 with the Polycomb complex is required for repression and regulation of myoblast differentiation. Furthermore, Msx1 promotes a dynamic spatial redistribution of the H3K27me3 repressive mark to the nuclear periphery in myoblast cells and the developing limb in vivo. Our findings illustrate a hitherto unappreciated spatial coordination of transcription factors with the Polycomb complex for appropriate regulation of gene expression programs during development.

INTRODUCTION

Appropriate spatial and temporal control of gene expression during development involves a coordinated network of chromatin-modifying complexes and sequence-specific DNA binding proteins, which operate within the dynamic spatial organization of the nucleus. Indeed, the nucleus is comprised of distinct functional and morphological compartments, such as those dedicated to transcription (Lanctôt et al., 2007; Misteli, 2007), and wherein chromosomes tend to be organized with gene-rich regions near the interior and gene-poor regions near the periphery (Fraser and Bickmore, 2007; Towbin et al., 2009; Zhao et al., 2009).

Among chromatin regulators, the polycomb repressive complexes, PRC1 and PRC2, act sequentially and coordinately to repress gene expression by covalent modification of chromatin (Schuettengruber and Cavalli, 2009). The PRC2 complex, which includes the enzymatic component, Ezh2, as well as Suz12 and EED, imparts a repressive trimethyl mark at lysine 27 of histone H3 (H3K27me3) (Cao et al., 2002; Kuzmichev et al., 2002; Schwartz and Pirrotta, 2007), associated with lineage commitment in embryonic stem cells and differentiation during development (Boyer et al., 2006; Bracken et al., 2006). PRC2 complexes are highly dynamic, tending to be active during developmental stages when cells are proliferating but not yet differentiated, and associated with genes that are repressed but poised for expression when differentiation ensues (Bracken et al., 2006; Ezhkova et al., 2009). This is exemplified in the myogenic lineage, where Ezh2 is expressed in myoblast cells but downregulated in myotubes, while its forced expression inhibits the formation of myotubes (Caretti et al., 2004). Although mammalian Polycomb response elements (PRE) have recently been identified (Mendenhall et al., 2010; Sing et al., 2009; Woo et al., 2010), how PRC2 complexes are recruited to genomic targets in dynamic spatial and temporal contexts has not been fully elucidated.

Homeoproteins comprise one of the major classes of transcriptional regulators that control differentiation during development. Among these, *Msx1* is expressed in diverse spatial and temporal domains during development, where a unifying feature is its restricted expression to proliferating cells that are poised to differentiate and its downregulation prior to differentiation (Bendall and Abate-Shen, 2000; Davidson, 1995). In the developing limb, for example, where *Msx1*, together with *Msx2*, is required for proper limb formation (Lallemand et al., 2005), *Msx1* is expressed in a zone of undifferentiated mesenchymal cells destined to form structural elements of the limb, but not in the adjacent cells differentiating to form these structures (Bendall et al., 1999; Catron et al., 1996; Davidson, 1995; Davidson

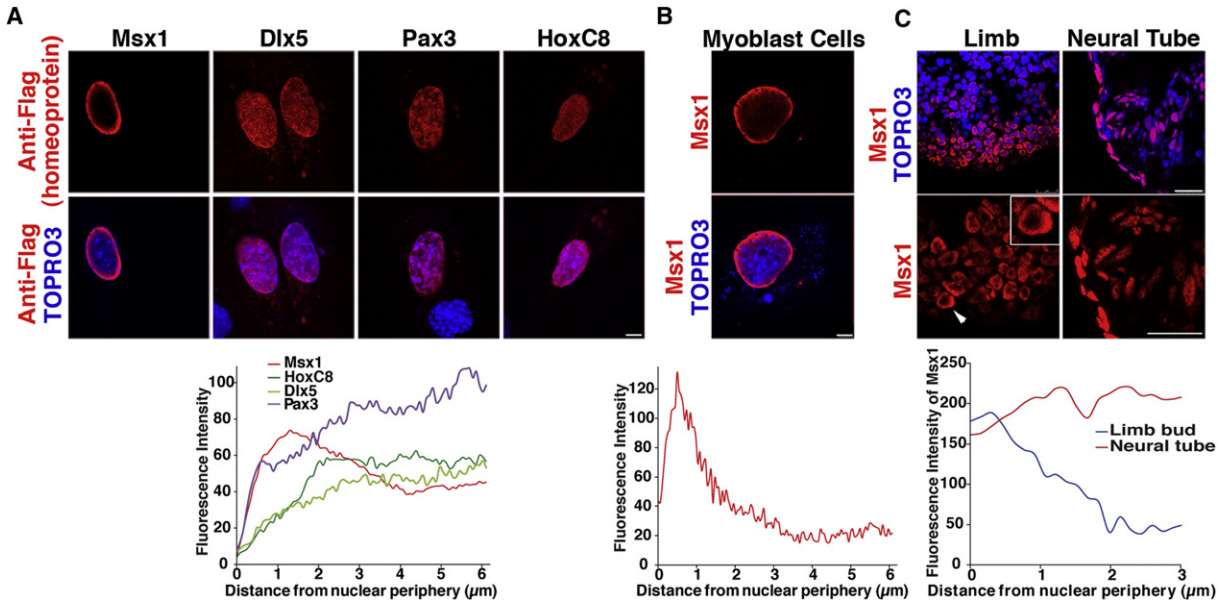

Figure 1. Msx1 Is Localized to the Nuclear Periphery

(A and B) Localization of Msx1, but not other homeoproteins, to the nuclear periphery in myoblast cells. C2C12 cells (A) or primary myoblasts (B) were transfected with plasmids encoding Flag-Msx1 or the indicated Flag-tagged homeoproteins and visualized by immunofluorescence. Localization was quantified using ImageJ software.

(C) Subnuclear localization of Msx1 in mouse development. Immunofluorescence staining of mouse embryos (10.5 days postcoitum [dpc]) shows enrichment of Msx1 at the nuclear periphery in the limb but not neural tube. Quantification of Msx1 localization was done using ImageJ; data are shown as a summary for 30 cells. Scale bars represent 5 μm (A and B) and 25 μm (C).

See also Figure S1A.

et al., 1991). Similarly, in the myogenic lineage Msx1 is expressed in myogenic precursors during development as well as in adult satellite cells (i.e., stem cells), but not in differentiated myotubes (Bendall et al., 1999; Cornelison et al., 2000; Houzelstein et al., 1999). Furthermore, forced expression of Msx1 in myoblast cells inhibits their differentiation (Hu et al., 2001; Woloshin et al., 1995), whereas its forced expression in myotubes results in their dedifferentiation (Odelberg et al., 2000). The inhibitory consequences of Msx1 for differentiation are mediated, in part, by its actions as a transcriptional repressor. For instance, Msx1 represses the expression of *MyoD*, a principal regulator of myogenic differentiation, by binding to the core enhancer region (CER) (Bendall et al., 1999; Lee et al., 2004; Lee et al., 2006; Woloshin et al., 1995), which regulates the timing of *MyoD* expression in vivo (Goldhamer et al., 1995). Notably, this interaction occurs at the nuclear periphery, and this subnuclear localization is required for repression by Msx1 (Lee et al., 2006).

In the current study, we investigate the consequences of Msx1 localization to the nuclear periphery for its function in transcriptional repression in myoblast cells and the murine embryonic limb. We identify Msx1 target genes and find that the repressed targets are preferentially located at the nuclear periphery in myoblast cells, where Msx1 is also located. We further show that their repression requires association of Msx1 with the PRC2 complex, resulting in an Msx1-dependent enrichment of H3K27me3 on Msx1 genomic binding sites as well as a striking redistribution of this repressive mark to the nuclear periphery. Our findings highlight a hitherto unappreciated role of spatial context of chromatin marks as a key factor in regulating gene expression during development.

RESULTS

Msx1 and Its Repressed Target Genes Are Located at the Nuclear Periphery in Myoblast Cells

We have shown previously that transcriptional repression by Msx1 in C2C12 myoblast cells requires its localization to the nuclear periphery (Lee et al., 2006). We now find that this striking localization of Msx1 to the periphery is distinctive, as it is not shared by other classes of homeoproteins (Figure 1A and see Figure S1A available online); notably, the C-terminal region of Msx1 that is required for localization to the periphery (Lee et al., 2006 and below) is not conserved with other homeoproteins (Bendall and Abate-Shen, 2000). Furthermore, this subnuclear localization by Msx1 also occurs in primary myoblasts in culture, as well as the developing limb of mouse embryos in vivo, but not in all other tissues where Msx1 is expressed during development, such as the neural tube (Figures 1B and 1C). Thus, localization to the nuclear periphery is a distinctive feature of Msx1 that occurs in specific biological contexts.

To further investigate the significance of this subnuclear localization for transcriptional regulation, we first identified Msx1 target genes and then assessed their subnuclear localization in myoblast cells. Target genes were identified using a combination of gene expression profiling and chromatin-immunoprecipitation followed by high-throughput sequencing (ChIP-Seq) to identify

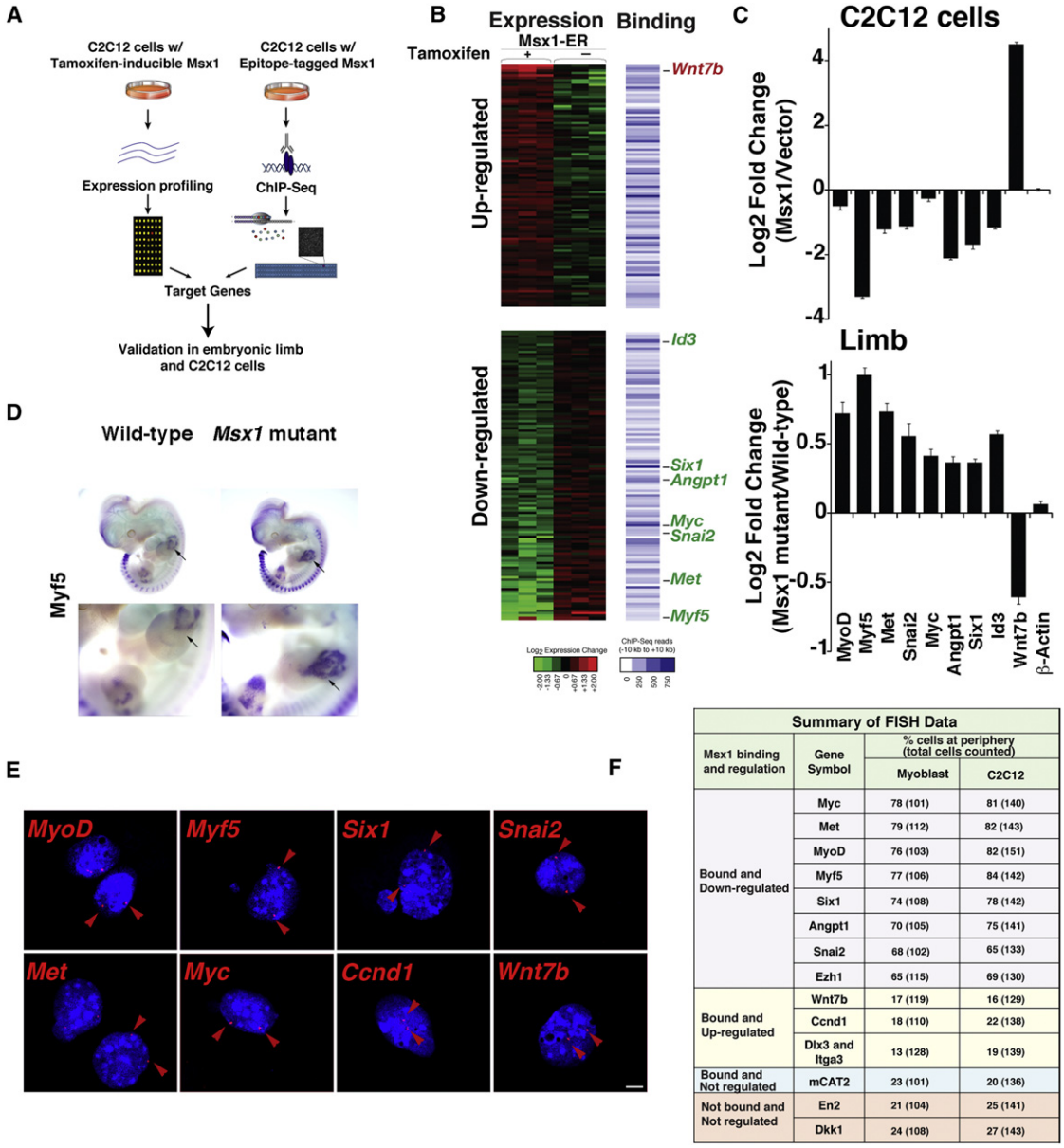

Summary of FISH Data

Msx1 binding and regulation	Gene Symbol	% cells at periphery (total cells counted)	
		Myoblast	C2C12
Bound and Down-regulated	Myc	78 (101)	81 (140)
	Met	79 (112)	82 (143)
	MyoD	76 (103)	82 (151)
	Myf5	77 (106)	84 (142)
	Six1	74 (108)	78 (142)
	Angpt1	70 (105)	75 (141)
	Snai2	68 (102)	65 (133)
	Ezh1	65 (115)	69 (130)
Bound and Up-regulated	Wnt7b	17 (119)	16 (129)
	Ccnd1	18 (110)	22 (138)
	Dlx3 and Itga3	13 (128)	19 (139)
Bound and Not regulated	mCAT2	23 (101)	20 (136)
Not bound and Not regulated	En2	21 (104)	25 (141)
	Dkk1	24 (108)	27 (143)

Figure 2. Repressed Target Genes Are Enriched in the Nuclear Periphery

(A) Strategy for identification of Msx1 target genes. Gene expression profiling was done in cells expressing tamoxifen-inducible Msx1 and ChIP-Seq analyses in cells expressing Flag-Msx1. Target genes were inferred as those bound and regulated by Msx1.

(B) Comparison of expression and binding data. Selected upregulated (red) or downregulated (green) genes are indicated.

(C) Real-time PCR of expression of selected target genes in C2C12 cells expressing or lacking Msx1 or the forelimb of *Msx1; Msx2* conditional mutant versus wild-type mice at 13.5 dpc.

(D) In situ hybridization of *Myf5* showing upregulation in the forelimbs of $Msx1^{-/-}$ mutant versus $Msx1^{+/+}$ mice at 11.5 dpc. Wild-type and mutant embryos were stained for the same amount of time to visualize differential levels of *Myf5* expression.

(E) Repressed target genes of Msx1 are localized to the nuclear periphery. FISH analyses showing the localization of the indicated genes in primary myoblast cells. Scale bar represents 5 μm.

(F) Summary of FISH data showing the percentage of cells localized at the nuclear periphery; data represent the summary of three independent experiments examining at least 100 cells. Values are the means ± standard deviation (SD).

See also Figure S1, Figure S2, and Tables S1–S3 and Table S4.

genes that are both differentially expressed and bound by Msx1 (Figure 2A). Because Msx1 is virtually undetectable in most cultured cells, including myoblasts (J.W. and C.A.-S., unpublished data), we performed these analyses in C2C12 cells expressing exogenous Msx1 (Hu et al., 2001; Lee et al., 2004; Lee et al., 2006), and then validated our findings for endogenous Msx1 in the developing limb, comparing *Msx1* mutant with wild-type embryos (Figure 2A).

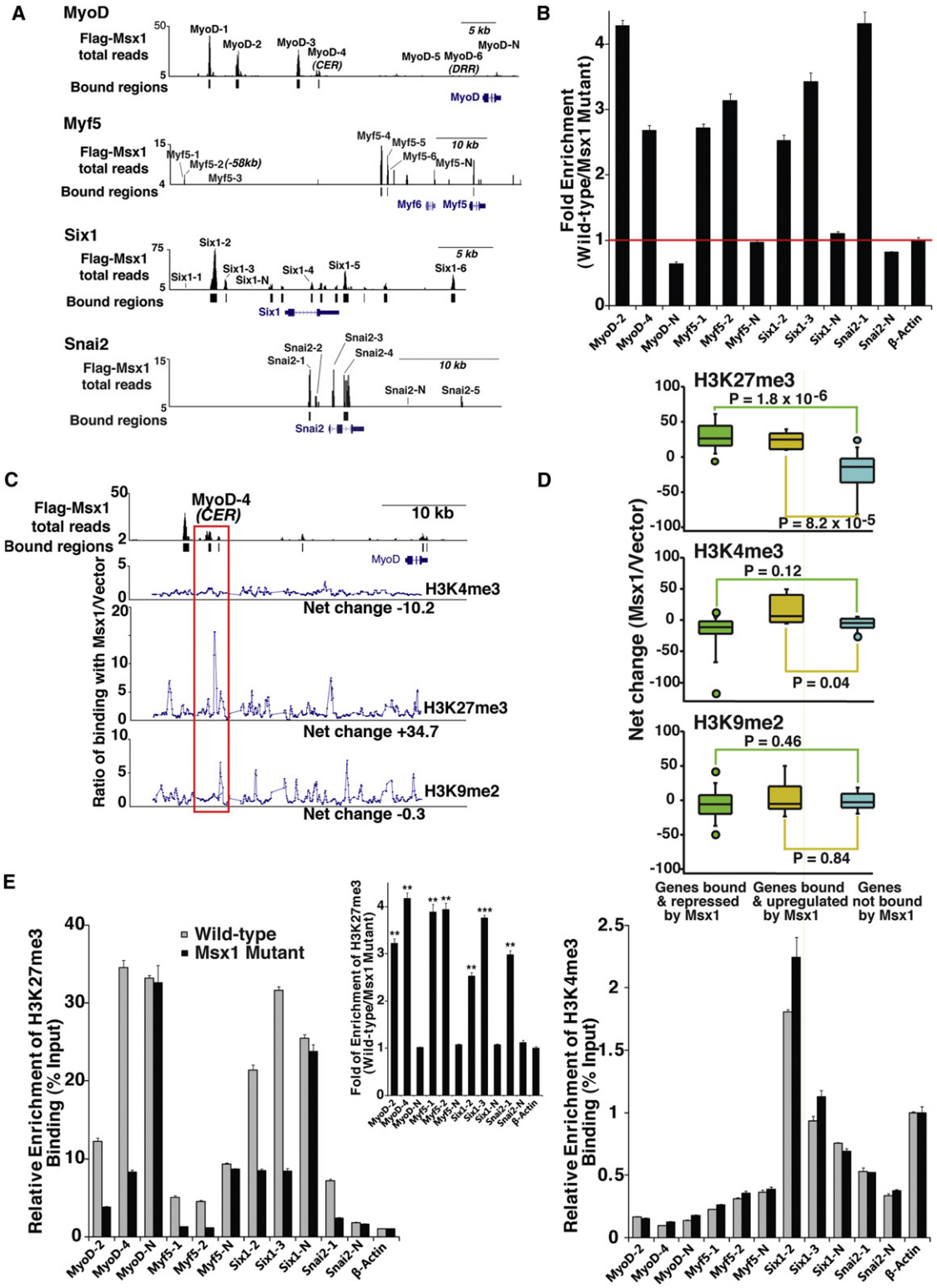

Figure 3. Msx1 Genomic Binding Leads to Enrichment of the H3K27me3 Repressive Mark

(A) ChIP-Seq binding plots for repressed target genes showing the sequence "reads" over the indicated genomic interval, and position of negative control regions not bound by Msx1 (i.e., MyoD-N, Myf5-N, Six1-N, and Snai2-N).

(B) ChIP-qPCR validation of binding by endogenous Msx1 in the forelimb (13.5 dpc) to indicated sites on target genes. ChIP assays, done with an Msx1 monoclonal antibody, compare the *Msx1*; *Msx2* conditional mutants with wild-type limbs; data are expressed as fold enrichment of Msx1 binding and normalized to input. ChIP-qPCR validation of exogenous Msx1 in C2C12 cells is shown in Figure S2H. The sequences of the binding regions are provided in Table S5.

We performed Affymetrix gene expression profiling using RNA from C2C12 cells expressing tamoxifen-inducible Msx1 (Hu et al., 2001), focusing on genes whose expression was differentially regulated shortly after (i.e., within 6 hr) induction to enrich for direct target genes (Table S1). We compared these with genes bound by Msx1 within 10 kb of the transcription start site (TSS), as determined by ChIP-Seq analyses of genomic DNA from C2C12 cells expressing a constitutively-active epitope-tagged Msx1 (Lee et al., 2006) (Figure S2A and Table S2). Comparison of differentially expressed genes (i.e., from the gene expression profiling data) with those bound by Msx1 (i.e., from the ChIP-Seq analyses) revealed 79 upregulated and 87 downregulated target genes (total of 166) (Figure 2B and Table S3). Although many more genes were bound by Msx1 (i.e., 8606 genes) than were differentially expressed (i.e., 221 genes), more than 75% of the differentially expressed genes were also bound by Msx1 ($p = 9.8 \times 10^{-10}$), and particularly the downregulated genes had a bias for Msx1 binding at or near the TSS ($p = 0.01$) (Figures S2B and S2C and Table S3). Interestingly, Msx1 genomic binding sites were enriched for its consensus DNA binding site (i.e., TAATT) (Figure S2D), while de novo motif discovery analyses revealed the prevalence of additional sequence motifs, including an AP1 binding site (see Supplemental Experimental Procedures and Figure S2E). Thus, recognition of target sequences by Msx1 in vivo may involve both direct and indirect interactions.

Consistent with the known functions of *Msx1* as a negative regulator of differentiation (Bendall and Abate-Shen, 2000), functional annotation of target genes revealed that those upregulated were enriched for genes involved in controlling the cell cycle, cellular proliferation, and/or development, whereas those downregulated tended to be involved in differentiation, bone remodeling, and/or myogenesis, as well as development (Figure S2F). We validated the differential expression of selected target genes, which were chosen on the basis of their potential relevance for myogenesis and/or differentiation, by real-time PCR using RNA from C2C12 cells expressing or lacking exogenous Msx1 (Figure 2C and Table S4). The differential expression of target genes was further validated in developing limbs of *Msx1* mutant versus wild-type embryos, using real-time PCR as well as in situ hybridization, which showed that genes downregulated in C2C12 cells expressing exogenous *Msx1* were upregulated in the mutant limb lacking *Msx1* and vice versa (Figures 2C and 2D, Table S4, and Figure S2G). Notably, our finding that target genes identified in C2C12 cells are also regulated by Msx1 in murine embryos indicates that they are indeed bona fide targets in vivo.

We next investigated the subnuclear localization of Msx1 target genes in myoblast cells using fluorescence in situ hybridization (FISH) analyses. We found that the genes bound and downregulated by Msx1 exhibited strong (i.e., *Myc*, *Met*, *MyoD*, and *Myf5* > 75%) or moderate (i.e., *Six1*, *Angpt1*, *Snai2*, and *Ezh1* > 65%) association with the nuclear periphery in both C2C12 and primary myoblast cells (Figures 2E and 2F and Figures S1B and S1C). Importantly, this was only the case for the repressed targets (i.e., the downregulated genes), because the genes that were bound and upregulated by Msx1, as well as other genes that were neither bound nor regulated by Msx1 were not preferentially associated with the nuclear periphery (Figures 2E and 2F and Figures S1B and S1C). As we had observed previously (Lee et al., 2006), the localization of target genes at the nuclear periphery was not dependent on expression of Msx1 (Figures 2E and 2F and Figures S1B and S1C). Because target genes that are repressed, but not activated, were localized to the nuclear periphery, our subsequent analyses to investigate the consequences of Msx1 localization to the nuclear periphery for transcriptional control in myoblast cells was focused primarily on the repressed target genes.

Msx1 Genomic Binding Is Associated with Enrichment of the H3K27me3 Repressive Mark

Consistent with the known functions of Msx1 as a transcriptional repressor and negative regulator of muscle cell differentiation (Hu et al., 2001; Lee et al., 2004, 2006; Odelberg et al., 2000; Woloshin et al., 1995), these repressed target genes include known regulators of muscle cell differentiation, such as *Six1*, *Snai2*, and *Myf5* (Figures 2B–2D and Table S4). Inspection of the ChIP-Seq binding data for these targets, as well that of a previously known target, *MyoD*, revealed Msx1 binding to multiple sites at these genes (Figure 3A and Table S5). Chromatin immunoprecipitation (ChIP) analyses of endogenous Msx1 in embryonic limb as well as exogenous Msx1 in C2C12 cells confirmed binding to these genomic sites, but not to other sites where Msx1 was not bound in the ChIP-Seq analyses (i.e., negative control sites) (Figure 3B and Figure S2H). Notably, these Msx1 genomic binding sites include regulatory regions such as the CER of *MyoD*, as well as the −58 kb distal regulatory element of *Myf5*, which are known homeoprotein-binding elements that control expression of these respective myogenic regulators in

(C) ChIP-Seq data for Msx1 compared with ChIP-Chip data for the indicated H3 marks on *MyoD* in C2C12 cells expressing or lacking Msx1; the red box shows the region corresponding to the *CER* (MyoD-4). The net change score indicates the relative increase (positive score) or decrease (negative score) of histone mark comparing the Msx1-expressing versus control cells. Comparable data for *Myf5* and *Six1* are shown in Figure S3A.

(D) Summary of the relative levels of H3K27me3, H3K4me3, and H3K9me2 at Msx1-repressed target genes and Msx1-upregulated target genes compared to genes not bound by Msx1. ChIP-Chip data from 15 genes bound-and-repressed by Msx1, 7 genes bound-and- activated by Msx1, and 15 comparable genes not bound by Msx1 were scored for the net change in the indicated chromatin marks over ~30 kb upstream of the transcription start site in C2C12 cells expressing versus lacking Msx1 (Msx1/vector). A positive score indicates a gain of that mark at the selected genes in Msx1-expressing cells relative to control cells, and a negative score indicates a loss. Significance was calculated using a Mann-Whitney U test, and p values are indicated on the figure. Whiskers on box plots show the 90th and 10th percentiles of the distributions.

(E) ChIP-qPCR analyses showing the relative levels of H3K27me3 or H3K4me3 at Msx1 genomic binding sites in *Msx1; Msx2* conditional mutant versus wild-type limb. ChIP data are expressed as relative enrichment of the H3 mark normalized to input. Inset: ChIP data expressed as fold enrichment in wild-type embryonic limb versus *Msx1*; *Msx2* conditional mutant embryonic limb (and normalized to input). Comparable data for exogenous Msx1 expressed in C2C12 cells is shown in Figure S4A. Values are the means ± SD. ***$p < 0.0001$; **$p < 0.001$; *$p < 0.01$.

See also Figures S2–S4, Table S5, and Table S6.

the developing limb (Buchberger et al., 2007; Goldhamer et al., 1995; Hadchouel et al., 2003).

In the course of these analyses, we noticed a significant overlap between target genes repressed by Msx1 and genes previously identified as Polycomb targets in mouse embryonic stem (ES) cells (34/87 genes; $p = 8.6 \times 10^{-6}$), as well as genes enriched for H3K27me3 in mouse ES cells (27/87 genes; $p = 2 \times 10^{-4}$) (Table S6) (Boyer et al., 2006; Mikkelsen et al., 2007). Considering these observations, as well as our previous findings showing that Msx1 genomic binding at the CER is correlated with increased levels of repressive chromatin marks at this site (Lee et al., 2004), we asked whether repressive chromatin marks were enriched on Msx1 target genes. We used chromatin immunoprecipitation coupled with DNA microarray hybridization (ChIP-Chip) to examine the relationship between Msx1 genomic binding and levels of the Polycomb mark, H3K27me3, as well as another repressive mark, H3K9me2, and a mark of active chromatin, H3K4me3 (Figure 3C and Figure S3A). These studies were done using a high-density array containing several hundred developmental regulatory genes, including Msx1 target genes (Supplemental Experimental Procedures) to evaluate the levels of these histone marks relative to Msx1 genomic binding in C2C12 cells expressing or lacking Msx1. These ChIP-Chip binding data revealed an Msx1-dependent overall enrichment of H3K27me3 on repressed target genes (*MyoD*, net change +34.7; *Myf5*, net change +23.2; *Six1*, net change +22.7), but no such enrichment of the H3K9me2 repressive mark or the H3K4me3 activator mark on these repressed genes (Figure 3C and Figure S3A).

More generally, the overall abundance of H3K27me3 on repressed Msx1-bound genes versus comparable genes not bound by Msx1 (N = 15/group) revealed a significant enrichment of H3K27me3 in Msx1-expressing cells (median net change +28.6; $p = 1.8 \times 10^{-6}$), which was not the case for H3K9me2 or H3K4me3 (Figure 3D). Interestingly, not only did we observe an increase in the H3K27me3 mark on repressed genes bound by Msx1, we observed a decrease in H3K27me3 levels on genes not bound by Msx1 (median net change −14; $p = 1.8 \times 10^{-6}$). In particular, *Dkk1* and *En2*, which are neither bound nor regulated by Msx1, had reduced levels of H3K27me3 in Msx1-expressing cells (net change, *Dkk1* −78.8; *En2* −85.8) (Figure S3B).

To rule out any potential bias due to selection of genes for these analyses, we examined the genomic loci for two *Hox* clusters, each spanning >100 kb, and found that the *HoxC* cluster, which is strongly bound by Msx1, was significantly enriched for H3K27me3 in Msx1-expressing cells (net change +383), whereas the *HoxD* cluster, which was virtually devoid of Msx1 binding, had reduced levels of H3K27me3 in Msx1-expressing cells (net change −174) (Figure S3C). Taken together, these findings suggest that Msx1 promotes the redistribution of the H3K27me3 mark from genomic regions where Msx1 is not bound to those where it is bound. Notably, enrichment of the H3K27me3 mark was also observed on genes that were activated, rather than repressed by Msx1 (median net change +24.9; $p = 8.2 \times 10^{-5}$) yet, unlike the repressed genes, the activated genes, which are not localized to the nuclear periphery, were also enriched for the H3K4me3 mark (median net change +6.3; $p = 0.04$) (Figure 3D and Figure S3A). Therefore, although Msx1 binding may promote enrichment of the H3K27me3 mark on target genes, whether the outcome is repression or activation may be influenced by the status of other histone marks, as well as the localization of targets within the nuclear compartment.

Further comparison of the ChIP-Seq binding data for Msx1 and the ChIP-Chip data for histone marks indicated that enrichment for H3K27me3 was particularly evident on genomic regions in proximity to, although not necessarily directly overlapping, the location of Msx1 binding sites, as exemplified for the CER (Figure 3C). This was validated by ChIP-qPCR in which we found the loss of Msx1 expression in mutant limbs resulted in reduced levels of H3K27me3 whereas the gain of Msx1 expression in C2C12 cells resulted in increased levels of H3K27me3 on Msx1-binding sites on target genes (Figure 3E and Figure S4A). For example, the levels of H3K27me3 were significantly reduced in the Msx1 mutant versus wild-type limb at the *MyoD* CER (MyoD-4; 4.2-fold; $p = 1.6 \times 10^{-4}$) and the −58 kb region of *Myf5* (Myf5-2; 3.9-fold; $p = 5.1 \times 10^{-4}$) but not at genomic sites not bound by Msx1 (i.e., the negative control sites), while the levels of the H3K4me3 mark did not vary any of these sites on the repressed genes as a consequence of Msx1 expression (Figure 3E); similar results were observed in C2C12 cells (Figure S4A). Conversely, genes that were neither bound nor regulated by Msx1 (i.e., *Mck*, *MHCIIb*, *Dkk1*, *En2*, and *Irx1*) had reduced levels of H3K27me3 in Msx1-expressing C2C12 cells (Figure S4B). These findings further underscore the observation that Msx1 promotes a redistribution of H3K27me3 to its bound genomic sites, and demonstrate that repressed target genes have increased levels of the H3K27me3 mark, particularly near genomic sites where Msx1 is bound.

Msx1 Associates with PRC2 via the Homeodomain and the C-Terminal Region

We next considered how binding by Msx1 results in enrichment of repressive chromatin marks on target genes. We found that the Msx1 protein complex immunopurified from C2C12 cells as well as the endogenous Msx1 complex immunopurified from embryonic limb have associated histone methyltransferase activity specific for histone H3 (Figure 4A). Notably, this histone methyltransferase enzymatic activity is associated with but not an inherent property of Msx1, because the recombinant protein (i.e., MBP-Flag-Msx1) is completely devoid of this activity (Figure 4A). This Msx1-associated histone methyltransferase activity has specificity for H3 lysine 27, because nucleosomes synthesized using an H3 variant lacking K27 were not optimal substrates (Figure 4B). Additionally, coimmunoprecipitation assays revealed that Msx1 associates with H3K27me3, but not with several other histone methyl marks (Figure 4C). Interestingly, we also observed associated histone methyltransferase activity for the closely related Msx2 homeoprotein, but not another homeoprotein, Dlx5, which functions as a transcriptional activator to antagonize the functions of Msx1 (Bendall and Abate-Shen, 2000; Zhang et al., 1997) (Figure S4C); notably, unlike Msx1, Dlx5 was not localized at the nuclear periphery (Figure 1A).

Furthermore, we found that Msx1 associates directly with components of the PRC2 complex, which imparts the H3K27me3 mark, including Ezh2, Suz12, and EED (Figure 4D). Notably, exogenous Msx1, from C2C12 cells, and endogenous Msx1, from developing limb, interacted strongly with the PRC2

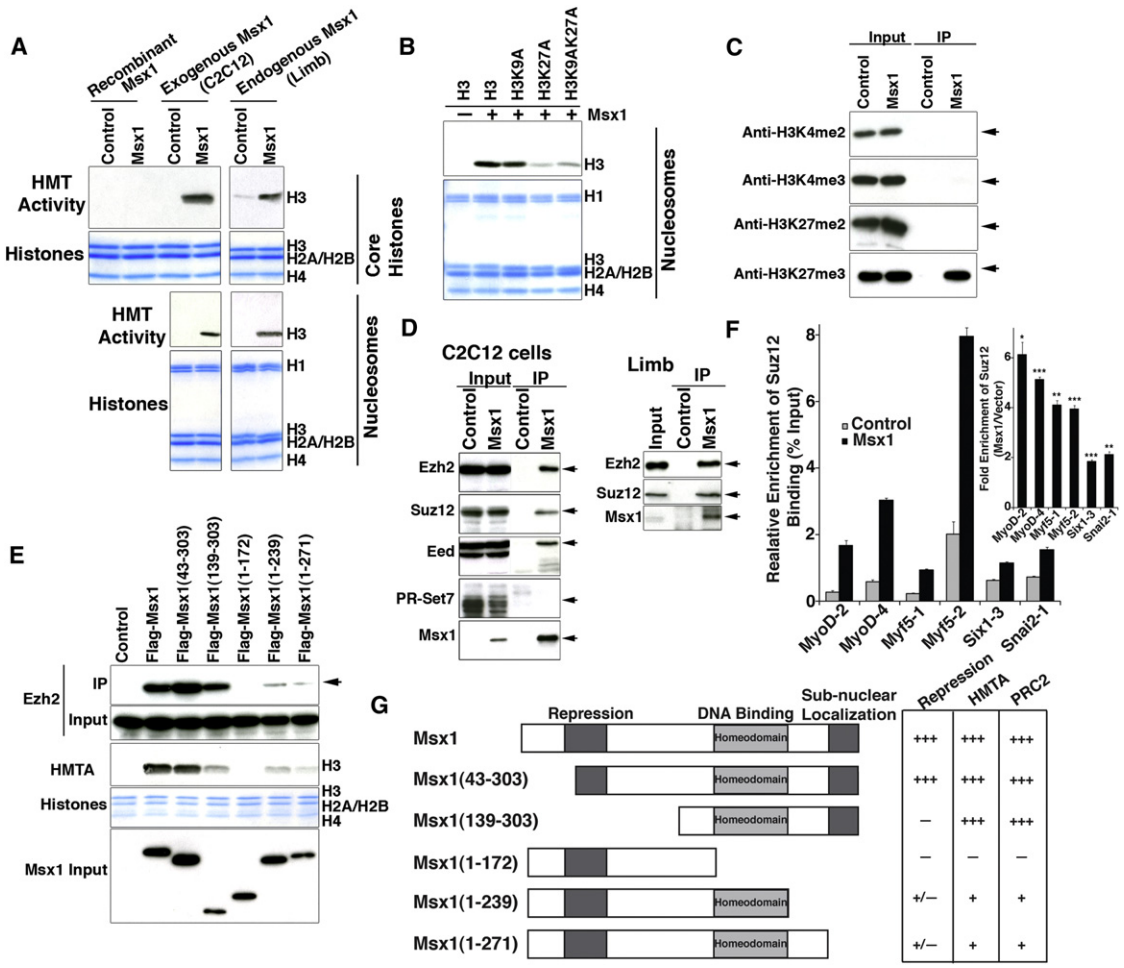

Figure 4. Msx1 Associates with PRC2 via the Homeodomain and C-Terminal Region

(A and B) Histone methyltransferase activity assays. Assays in (A) were done with recombinant Msx1 protein or the immunopurified Msx1 protein complex from C2C12 cells (exogenous Msx1) or embryonic limb (endogenous Msx1) with core histones or nucleosomes as substrate. Assays in (B) done with immunopurified Msx1 from embryonic limb using nucleosomes synthesized with H3 variants having alanine substitutions for K9 and/or K27 as indicated. Histone methyltransferase activity was measured by incorporation of radioactive S-adenosylmethionine and visualized by autoradiography. Core histones are shown by Coomassie blue staining.

(C and D) Coimmunoprecipitation assays. Assays in (C) were done using C2C12 protein extracts expressing Flag-Msx1 and were immunoprecipitated with anti-Flag followed by immunoblotting for the indicated histone marks. Assays in (D) were done using protein extracts from C2C12 cells expressing Flag-Msx1 and immunoprecipitated with anti-Flag or with extracts from embryonic forelimb (11.5 dpc) and immunoprecipitated with anti-Msx1 antibody (4F11) following by immunoblotting for the indicated PRC2 subunits or other proteins as indicated.

(E) Domain mapping analyses. 293T cells expressing Flag-Msx1 or the indicated truncated Flag-Msx1 protein complexes were immunopurified with anti-Flag followed by immunoblotting to detect Ezh2 or assayed for histone methyltransferase activity.

(F) ChIP-qPCR assays were done using C2C12 cells expressing or lacking Msx1 to evaluate binding of Suz12 to the indicated Msx1 target sequences. ChIP data are expressed as relative enrichment of Suz12 binding normalized to input. Inset: ChIP data expressed as fold enrichment of Suz12 binding in C2C12 cells expressing exogenous Msx1 versus the control cells (and normalized to input).

(G) Schematic representation of Msx1 and truncated derivatives showing a summary of data. Values are the means ± SD. ***$p < 0.0001$; **$p < 0.001$; *$p < 0.01$. See also Figure S4.

complex, regardless of whether coimmunoprecipitation assays were done using antibodies to pull down Msx1 or Ezh2 (Figure 4D and Figure S4D). In contrast, Msx1 did not interact with other histone methyltransferases, such as PR-SET7, which are associated with marks of heterochromatin silencing rather than repression (Margueron and Reinberg, 2010) (Figure 4D).

By analyses of truncated Msx1 proteins, we found that the homeodomain is required for association with the histone methyltransferase enzymatic activity, as well as interaction with the PRC2 complex (Figures 4E and 4G); notably, although the homeodomain mediates DNA binding, it also serves as a protein interaction domain for Msx1 (Bendall and Abate-Shen, 2000; Bendall et al., 1999; Zhang et al., 1996, 1997). Interestingly, the C-terminal region of Msx1 is also necessary for efficient association of Msx1 with histone methyltransferase activity and association with Ezh2 (Figures 4E and 4G); while this C-terminal region is not required for DNA binding it is necessary for localization of Msx1 to the nuclear periphery (Lee et al., 2006 and see below).

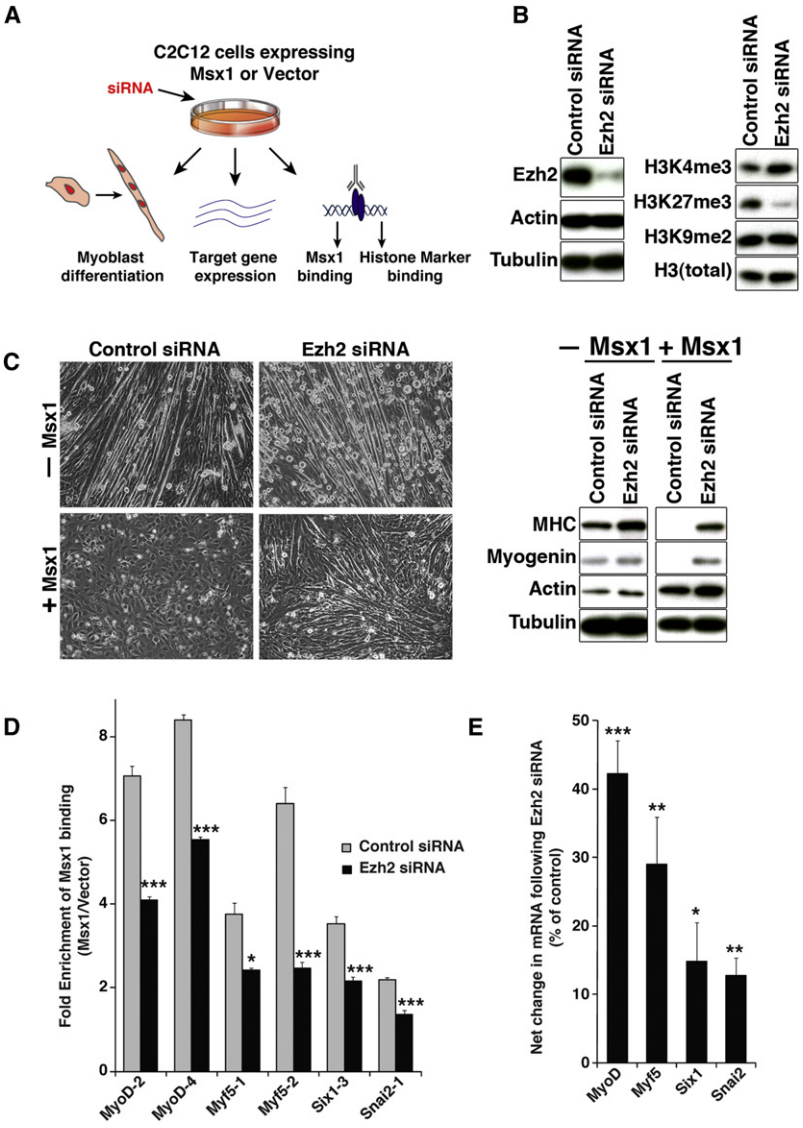

Figure 5. Functional Consequences of Msx1 Interaction with Ezh2 in Myoblast Cells

(A) Schematic diagram showing the strategy for analyzing the functional consequences of Ezh2 knock-down for Msx1 functions in myoblast cells. Data are shown for one Ezh2 siRNA; data with the second siRNA for Ezh2 is shown in Figure S5.

(B) Western blot assay showing reduced Ezh2 and the corresponding repressive mark H3K27me3 in cells with the Ezh2 siRNA.

(C) Differentiation assay of C2C12 cells expressing (+) or lacking (–) exogenous Msx1 along with siRNA for Ezh2 or a control siRNA. Left: Micrographs show the absence of myotubes in Msx1-expressing cells but not in cells also expressing the Ezh2 siRNA. Right: Western blot of markers of terminal muscle differentiation, MHC and Myogenin showing restored expression in the Msx1-expressing cells with the Ezh2 siRNA.

(D) ChIP-qPCR analyses showing relative Msx1 binding in C2C12 cells expressing exogenous Msx1 or a control as well as a control siRNA, or an Ezh2 siRNA. ChIP data are expressed as fold enrichment of Msx1 binding in C2C12 cells expressing exogenous Msx1 versus the control cells.

(E) mRNA expression levels of Msx1 target genes in cells with the Ezh2 siRNA or the control. Data are expressed as the net change of mRNA level relative to that control cells. Values are the means ± SD. ***$p < 0.0001$; **$p < 0.001$; *$p < 0.01$.

See also Figure S5.

Finally, we found that Msx1 binding to its repressed target genes was correlated with recruitment of PRC2 complexes to these genes (Figure 4F). In particular, ChIP-qPCR analyses revealed that Suz12 binding was significantly enriched at multiple Msx1 genomic binding sites, including known regulatory elements such as the CER (MyoD-4, 5.1-fold enrichment; $p = 1.2 \times 10^{-6}$) and the −58 kb site of *Myf5* (Myf5-2, 4.0-fold enrichment; $p = 1 \times 10^{-5}$) (Figure 4F). Collectively, these data suggest that the observed increase of H3K27me3 on Msx1 target genes reflects the recruitment by Msx1 of Polycomb complexes, as mediated by the homeodomain and facilitated by its C-terminal region.

Msx1 Association with PRC2 Complexes Is Necessary for Myoblast Differentiation and Repression of Myogenic Targets

We investigated the functional consequences of the interaction of Msx1 with the PRC2 complex using the strategy illustrated in Figure 5A. In particular, we introduced an Ezh2 (or a control) siRNA in C2C12 cells expressing Msx1 (or vector) and evaluated the consequences for: (1) differentiation, via appearance of myotubes and western blot detection of markers of terminal muscle differentiation, namely myosin heavy chain (MHC) and Myogenin; (2) target gene expression, via real-time PCR of mRNA levels; and (3) ChIP-qPCR analyses to evaluate binding of Msx1 or relevant histone marks at target genes (Figure 5 and Figure S5). We used two independent siRNAs for Ezh2 and verified their efficacy and specificity by western blotting for Ezh2 or histone marks, q-PCR analyses of *Ezh2* mRNA levels, and immunofluorescence detection of Ezh2 in C2C12 cells (Figure 5B and Figure S5A).

As we have shown previously (Hu et al., 2001; Lee et al., 2004; Lee et al., 2006), exogenous Msx1 completely abrogates differentiation of C2C12 cells, as evident by the absence of myotubes and lack of expression of MHC and Myogenin in cells expressing Msx1 compared to those lacking Msx1 (Figure 5C). In contrast, cells expressing Msx1 plus an Ezh2 siRNA were not inhibited for differentiation, as evident from the appearance of myotubes and expression of MHC and Myogenin (Figure 5C). Notably, Ezh2 knock-down significantly reduced Msx1 binding to genomic sites of repressed genes, as exemplified for the CER (MyoD-4, 3-fold reduced; $p = 1 \times 10^{-7}$) and the −58 kb element of *Myf5* (Myf5-2, 4-fold reduced; $p = 6.6 \times 10^{-5}$) (Figure 5D), suggesting that the PRC2 complex contributes to the efficacy of Msx1 binding to target genes. Notably, the diminished binding of Msx1 to repressed genes as a consequence of Ezh2 knock-down was accompanied by a partial

abrogation of their repression (Figure 5E and Figure S5B) as well as a significant reduction in H3K27me3, but not H3K4me3, as exemplified for the CER (MyoD-4, 4-fold reduced, $p = 1 \times 10^{-6}$) and the −58 kb region of *Myf5* (Myf5-2, 5.7-fold reduced, $p = 1.5 \times 10^{-5}$) (Figure S5C). Collectively, these findings demonstrate that interaction of Msx1 with the PRC2 complex in myoblast cells is essential for Msx1 to regulate myogenic differentiation, to bind and repress myogenic target genes, and for enrichment of histone repressive marks at Msx1 genomic binding sites.

Msx1 Redistributes the H3K27me3 Repressive Mark to the Nuclear Periphery

Although enriched on Msx1 target genes (see Figure 3), the overall levels of H3K27me3 remain relatively constant regardless of the status of Msx1 expression in C2C12 cells or the developing limb (Figure S6A); this is consistent with the results from the ChIP-Chip analyses showing that H3K27me3 is redistributed from genomic regions where Msx1 is not bound to regions bound by Msx1 (see Figure 3D). A hint as to how Msx1 might redistribute rather than increase the levels of H3K27me3 was provided by our observation that association of Msx1 with Ezh2 is augmented by the C-terminal region (Figures 4E and 4G), which is required for localization of Msx1 to the nuclear periphery (Lee et al., 2006). Therefore, we investigated whether Msx1 affected the spatial localization of Ezh2 and the H3K27me3 repressive mark within the nuclear compartment.

Indeed, we found that Ezh2 and H3K27me3 exhibited a striking Msx1-dependent localization to the nuclear periphery in both C2C12 and primary myoblast cells (Figures 6A–6C, Figures S6B, and Figures S7A and S7B). In particular, whereas Ezh2 and H3K27me3 were distributed throughout the nucleus in myoblast cells lacking Msx1, in cells expressing Msx1, they overlapped with Msx1 at the periphery in C2C12 and primary myoblast cells (N = 20 cells/experiment; three independent experiments) (Figures 6A–6C, Figure S6B, and Figures S7A and S7B). Interestingly, in nonmyoblast cells Ezh2 and H3K27me3 were not localized to the nuclear periphery irrespective of Msx1 expression or localization (Figure S6D). Furthermore, this colocalization with Msx1 at the nuclear periphery was specific for H3K27me3, because the subnuclear localization of H3K4me3 did not vary as a consequence of Msx1 expression (Figure S6C). Therefore, Ezh2 and H3K27me3 specifically colocalize with Msx1 in myoblast cells.

The requisite protein domains of Msx1 responsible for recruitment of Ezh2 and H3K27me3 to the nuclear periphery were those that mediate its association with Ezh2, its transcriptional repression, and its localization to the nuclear periphery. Therefore, Ezh2 and H3K27me3 colocalized at the nuclear periphery with wild-type Msx1 or Msx1 (43-303), but not with Msx1 proteins that were not active in transcriptional repression (i.e., Msx1 [139-303] and Msx1-A) or not localized to the nuclear periphery (i.e., Msx1 [1-271]) (Figures 6A–6C, Figure S6E, and Figures S7A and S7B). As expected, the Msx1-dependent accumulation of H3K27me3 at the nuclear periphery required Ezh2, because in Msx1-expressing cells depleted for Ezh2, the residual H3K27me3 was distributed throughout the nucleus rather than localized to the periphery, whereas the localization of H3K4me3 was not effected (Figure S6F).

Finally, we examined the localization of the H3K27me3 repressive mark in Msx1-expressing cells in the developing embryo, focusing on the limb bud where Msx1 is robustly expressed (Bendall and Abate-Shen, 2000) and localized to the nuclear periphery (see Figure 1C). In particular, in the anterior region of the limb bud where Msx1 is expressed, the H3K27me3 mark was localized to the nuclear periphery in most cells (94%; N = 192 cells). In striking contrast, in *Msx1* germline mutant limbs, the H3K27me3 mark was diffusely localized throughout the nucleus and only in a few cells was localized to the nuclear periphery (8%; N = 203 cells) (Figures 7A and 7B). To rule out the possibility that the observed shift in H3K27me3 localization in the germline mutant mice was not directly attributed to *Msx1* loss of function, we also examined an *Msx1; Msx2* conditional mouse allele in which targeted deletion was induced 2 days prior to analyses (Supplemental Experimental Procedures). Inspection of these *Msx1; Msx2* conditional mice showed that the majority of cells (>90%; N = 200) displayed the H3K27me3 mark throughout the nucleus rather than localized to the nuclear periphery (Figures 7A and 7B). These findings demonstrate that the observed enrichment of H3K27me3 at the nuclear periphery is a consequence of Msx1 expression, and further suggest that this localization is dynamic, because the redistribution of H3K27me3 in the limb bud was evident just 2 days after deletion of *Msx1; Msx2* in the conditional mice. Cumulatively, these studies demonstrate that Msx1 expression results in a dynamic shift of the H3K27me3 repressive mark to the nuclear periphery in precise developmental contexts.

DISCUSSION

Despite substantial advances in our understanding of the global role of epigenetic regulators in controlling gene expression programs and cell lineage decisions during development, considerably less is known about how these activities are integrated with sequence-specific transcription factors or how these various activities are coordinated within the nucleus. We now demonstrate that transcriptional repression and regulation of differentiation by the Msx1 homeoprotein requires recruitment of the Polycomb complex to repressed target genes located at the nuclear periphery. Furthermore, we find that in specific developmental contexts, Msx1 promotes the dynamic redistribution of a Polycomb repressive mark to the nuclear periphery in vivo (Figure 7C). Our findings suggest that repression by Msx1 during development is intimately linked with its ability to dynamically orchestrate the integration of these various activities at the nuclear periphery in appropriate spatial and temporal contexts.

Considering that Msx1 is localized to the nuclear periphery, the simplest interpretation of our findings is that Msx1 recruits the PRC2 Polycomb complex to repressed target genes, which are located at the periphery, where Polycomb catalyzes the H3K27me3 repressive mark on chromatin in the vicinity of Msx1 binding (Figure 7C). However, given the mutual dependence of Msx1 and PRC2 complexes for both repression and binding to genomic targets, as well as the characteristic binding promiscuity of homeoproteins, including Msx1 (Bendall and Abate-Shen, 2000), it seems more likely that the Polycomb complex is playing a more active role for both target gene selection

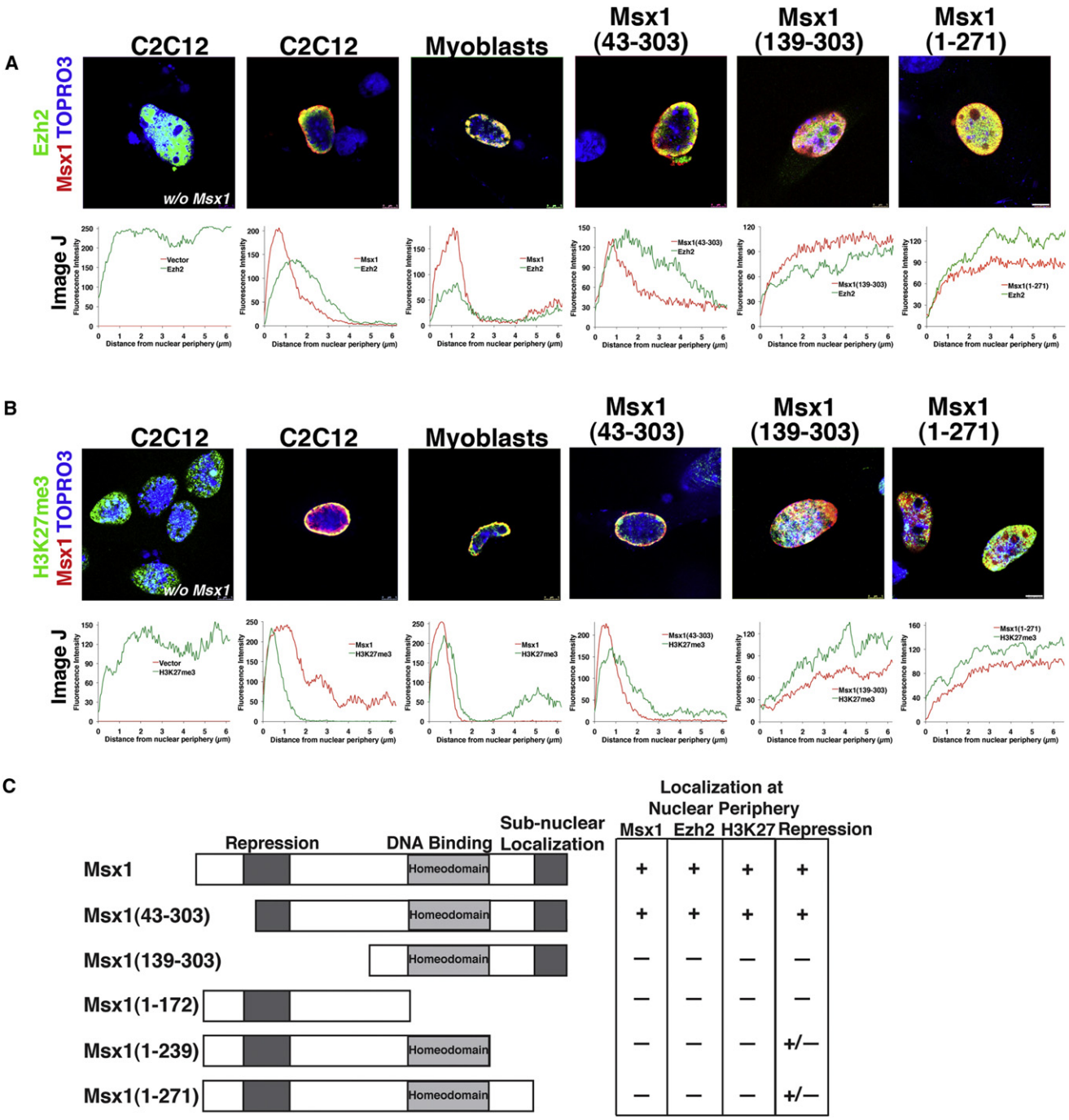

Figure 6. Ezh2 and H3K27me3 Colocalize with Msx1 at the Nuclear Periphery in Myoblast Cells

(A and B) Immunofluorescence assays were done on C2C12 cells or primary myoblast cells, expressing exogenous Ezh2 and Msx1 or the indicated Msx1 derivatives, and detected by immunofluorescence as indicated; TOPRO3 is marker of DNA. Quantitative analyses with ImageJ show representative data from three independent assays, each counting a minimum of 20 cells per variable. Scale bars represent 5 μm.

(C) Data summary.

See also Figure S6 and Figure S7.

and repression by Msx1. Furthermore, although this scenario may be relevant for transcriptional repression, additional complexity is suggested by the observations that Msx1 can function as an activator in certain cellular contexts (Hu et al., 2001) and that its target genes include many that are upregulated rather than repressed. Interestingly, while these activated genes are enriched for the H3K27me3 mark, they are also enriched for the activator mark H3K4me3, and are not located at the nuclear

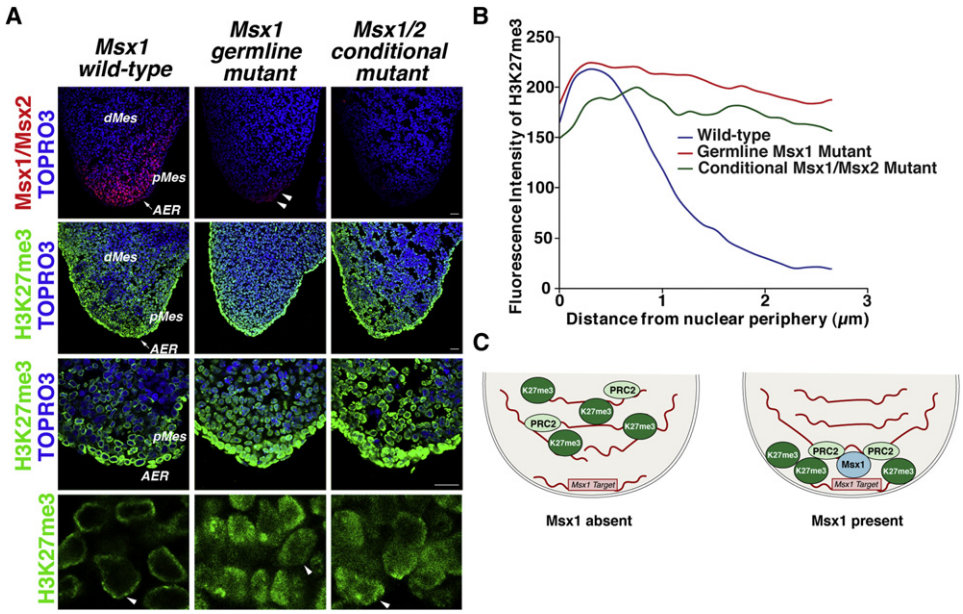

Figure 7. Msx1 Redistributes the H3K27me3 to the Nuclear Periphery In Vivo

(A) Immunofluorescence staining shows that in the developing mouse forelimb, H3K27me3 is enriched at the nuclear periphery where Msx1 is expressed but is not enriched at the periphery in limbs from *Msx1* germline or *Msx1; Msx2* conditional mutants. Scale bar represents 25 μm.

(B) Quantification of the H3K27me3 mark at the nuclear periphery from (A) was evaluated by ImageJ; data are shown for a summary of 30 cells.

(C) Working model. Discussed in the text.

periphery. Indeed, it has been shown recently that repositioning of *MyoD* to the nuclear interior is associated with its activation and binding of TAF3 during myoblast differentiation (Yao et al., 2011). Therefore, whether a target gene is "activated" or "repressed" may depend on its subnuclear localization as well as the distribution of activator and repressor chromatin marks and components of the core transcriptional complex.

Implicit in the model that repression by Msx1 involves recruitment of Polycomb to the nuclear periphery (Figure 7C) is that an important element of regulation should include the temporally controlled displacement of Msx1-PRC2 complexes from target genes and at least the partial reversal of the H3K27me3 mark as differentiation proceeds. Notably, UTX, which mediates the demethylation of H3K27me3, has been shown to be recruited to muscle-specific genes coincident with activation of their expression (Seenundun et al., 2010). Interestingly, in the skin Ezh2 has been shown to spatially regulate the timing of differentiation by inhibiting the binding of AP-1 transcriptional activators coincident with the onset of differentiation (Ezhkova et al., 2009). Notably, our ChIP-Seq analyses of Msx1 in myoblast cells revealed that Msx1 genomic binding sites are enriched for AP-1 consensus DNA sites; thus, is it plausible that this relationship of Ezh2 binding and AP-1 transcriptional regulation may occur in other cell lineages.

The Msx1 homeoprotein and the PRC2 Polycomb complex are active in similar biological contexts during development. Indeed, their expression tends to be temporally restricted to cells that are poised to differentiate and they each function to repress the expression of lineage regulators, and are inactivated prior to the onset of differentiation and subsequent activation of such lineage regulators (Bendall and Abate-Shen, 2000; Boyer et al., 2006; Bracken et al., 2006; Caretti et al., 2004; Ezhkova et al., 2009; Schuettengruber and Cavalli, 2009). Notably, a member of a distinct class of sequence-specific developmental regulators, GATA-1, has been shown to interact with PRC2 complexes in erythroid cells, where it controls the regulation of genes involved in erythroid development (Yu et al., 2009). Thus, interactions of the PRC2 Polycomb complex with tissue-specific developmental transcription factors may prove to be a general feature of how this chromatin complex achieves the dynamic spatial and temporal control of lineage-specific target genes in diverse cell types during development.

The biological significance of the coordinate actions of Msx1 and the PRC2 Polycomb complex is further evident because Msx1 and Polycomb share similar target genes, even in comparing distinct cell lineages (i.e., myoblast cells and ES cells), suggesting that there are universal aspects of their coordinate functions that extend beyond the biological model systems studied herein. Indeed, the interaction of Msx1 with Ezh2 is mediated by the homeodomain, which is the defining feature of this class of developmental transcription factors. Because the localization of Msx1 to the nuclear periphery is distinct among homeoproteins, it is conceivable that other homeoproteins may interact with Polycomb, but perhaps in other nuclear compartments.

Finally, our studies suggest a hitherto unappreciated level of transcriptional regulatory control during development, namely the spatial coordination of repressive chromatin marks within the nuclear compartment as a consequence of the functions of sequence-specific transcriptional regulators. Thus, although it is now widely accepted that the nucleus is organized into distinct "neighborhoods" (Fraser and Bickmore, 2007), whether

relocation between neighborhoods provides an active component of transcriptional regulation has not been resolved. Our findings provide biological evidence for relocation of repressor marks as contributing factor in regulating gene expression programs during development. In the broadest sense, our findings suggest that transcriptional repression can be viewed not only as a consequence of the dynamic control of chromatin modifications but also the result of "locating" repressive marks to appropriate spatial domains within the nucleus.

EXPERIMENTAL PROCEDURES

Description of Plasmids

Most plasmids used in this study have been described previously (Lee et al., 2004, 2006; Hu et al., 2001; Kuzmichev et al., 2004). Flag-tagged Ezh2 was generated from the corresponding cDNAs by PCR amplification using primers that introduced BamHI and XhoI sites for cloning into pcDNA3. All plasmids used were sequence verified.

Cell Culture Analyses

Cell culture studies were done using human 293T cells or mouse C2C12 myoblast or 3T3 fibroblast cells obtained from ATCC. Primary myoblasts were made from newborn (day 0) mouse limbs from Swiss Webster mice and maintained in F-10/DMEM growth medium. Other cells were maintained in DMEM supplemented with 10% fetal bovine in humidified atmosphere with 5% CO_2 at 37°C. Differentiation of C2C12 cells was induced by shifting cells to media containing 2% horse serum for 1–4 days (Lee et al., 2004, 2006). Exogenous Msx1 (or the control vector) was introduced either via retroviral gene transfer or by transient transfected as in (Lee et al., 2004, 2006). siRNA (Ambion) was introduced by transient transfection using the Lipofectamine RNAiMAX reagent (Invitrogen) according to the manufacturer's recommendations. The sequences of the siRNAs used in these studies are provided in Supplemental Experimental Procedures.

Analyses of *Msx1* Mutant Embryos

Forelimbs were analyzed from midgestation mouse embryos (staged 10.5–13.5 days postcoitum [dpc]) from: (1) Swiss Webster embryos; (2) germline *Msx1* mutant embryos (Satokata and Maas, 1994), comparing the homozygous null with homozygous wild-type embryos; or (3) conditional *Msx1; Msx2* mutants (Fu et al., 2007) crossed with an inducible $Rosa^{CreERT2}$ (Ventura et al., 2007). Targeted deletion of the conditional *Msx* alleles were induced by delivery of tamoxifen in corn oil (2 mg/40 g; Sigma-Aldrich) by oral gavage at embryonic day 9.5 (9.5 dpc) and confirmed in the tissue of interest (i.e., the limb) by PCR analyses. Embryos were collected from timed mating with noon on the day of the plug considered to be embryonic day 0.5; embryos were genotyped from yolk sac DNA.

Gene Expression Profiling Analyses

Gene expression profiling was done using RNA from C2C12 cells expressing tamoxifen-regulated Msx1 (Hu et al., 2001) or with empty vector as a control, followed by induction with 0.2 nM of tamoxifen or vehicle (DMSO) for 6 hr, and hybridized to Affymetrix GeneChips (Mu74AV2). Genes with a p value of ≤ 0.05 and a fold-change of ≥ 1.4-fold between tamoxifen-treated and vehicle samples for the Msx1-ER-infected cells were considered to be differentially expressed.

Validation of Target Gene Expression

Validation of differentially expressed genes was done using RNA from C2C12 cells or from embryonic forelimb isolated with Trizol reagent (Invitrogen) and purified using an RNeasy kit (QIAGEN). First strand cDNA was synthesized using SuperScript III kit (Invitrogen) and quantitative real-time PCR was performed using SYBR green reagent (QIAGEN) in the Realplex^2 machine (Eppendorf). Expression values were normalized to GAPDH. Four independent experiments were performed for each target gene. The average values are given as the mean ± standard deviation (SD). Primer sequences for real-time PCR are provided in Supplemental Experimental Procedures.

ChIP-Seq Analyses and Identification of Msx1 Target Genes

ChIP-Seq analysis was done using cross-linked chromatin from C2C12 cells expressing exogenous Flag-Msx1 by Solexa sequencing of immunoenriched DNA as in (Marson et al., 2008). Briefly, 5×10^7 cells were lysed and chromatin was sheared in lysis buffer (1 mM EDTA, 0.5 mM EGTA, 10 mM Tris-HCl [pH 8.0], 100 mM NaCl, 0.1% Na-Deoxycholate, 0.5% N-lauryl sarcosine) and then immunoprecipitated overnight with anti-Flag M2 antibody (Sigma-Aldrich, F3165). The immunoprecipitated protein-DNA complexes were recovered using Dynal Protein G beads, washed with RIPA buffer (0.1% SDS, 1% Na-Deoxycholate, 1% Triton X-100, 150 mM NaCl, 10 mM Tris-HCl [pH7.5], 1 mM EDTA, and protease inhibitor cocktail) and the protein-DNA complexes were eluted and reversed by heating at 65°C for 12 hr. Following purification, the recovered DNA was amplified and prepared for sequencing according to published methods (Marson et al., 2008).

Regions of DNA bound by Msx1 were identified using a Poissonian background model as described (Marson et al., 2008). Analysis of 5.2 million uniquely aligning reads identified 62,248 bound regions called at a p value threshold of 10^{-8}, which is listed in Table S2. Genes with a transcriptional start site (TSS) within 10 kb of an Msx1-bound region were called as bound by Msx1, resulting in 8606 bound genes. The identity and genomic coordinates of genes with start sites within 10 kb of Msx1-bound regions are listed in Table S2.

Target genes were identified by comparing the set of 8606 bound genes identified from the ChIP-Seq data to the set of 221 genes whose expression was changed (up- or downregulated) upon Msx1 induction in the gene expression profiling data to provide the list of 166 bound and regulated genes shown in Table S3. Gene ontology analysis was performed using the program DAVID v6.7 (http://david.abcc.ncifcrf.gov/home.jsp).

ChIP-Chip Analysis

ChIP-Chip analysis was done as in (Boyer et al., 2006) using cross-linked chromatin from C2C12 cells expressing Flag-Msx1 (or a control) on custom-designed Agilent arrays (see Supplemental Experimental Procedures). Immunoprecipitations were done using antibodies specific for histone marks H3K4me3, H3K27me3, or H3K9me2; details of all antibodies are provided in Supplemental Experimental Procedures.

ChIP-qPCR Assays

Chromatin immunoprecipitation (ChIP) assays were performed using cross-linked DNA from C2C12 cells or from embryonic limb as in (Lee et al., 2004, 2006). Quantitative PCR was performed in triplicate using SYBR green reagent (QIAGEN) in the Realplex^2 machine (Eppendorf). A minimum of three independent experiments were performed for each ChIP assay; the average values are given as the mean ± SD. Comparison of the differences between variables in each experiment were carried out by the two-tailed independent Student's t test. Unless otherwise indicated, real-time PCR data were normalized to input sample and fold enrichment relative to the input is indicated. The antibodies used for ChIP analyses and the primer sequences for the real-time PCR are provided in Supplemental Experimental Procedures.

Whole-Mount In Situ Hybridization

For in situ hybridization analyses, embryos were fixed in 4% PFA at 4°C for 16 hr, Whole-mount in situ hybridization was performed as described using digoxigenin (DIG)-labeled RNA probes (Bendall et al., 1999). Embryos were photographed using an Olympus SZX16 stereomicroscope equipped with an Olympus DP71 color digital camera. In situ analyses were done on a minimum of three mutant and three wild-type embryos at three embryonic stages (i.e., 10.5 to 13.5 dpc) in four independent experiments; in all cases, mutant and wild-type embryos were stained for exactly the same time to allow for comparison of expression levels.

Immunofluorescence Analyses

For immunofluorescence, cells were fixed in 4% PFA in PBS, permeabilized by incubation in 0.5% Triton X-100, and incubated with primary antibodies followed by AlexaFluor 488 and/or AlexaFluor 555 secondary antibodies (Molecular Probes). Immunofluorescence analyses of *Msx1* germline mutant, *Msx1; Msx2* conditional mutant, and wild-type limbs were done on 8 μm cryosections from PFA-fixed OCT blocks mounted on Superfrost positively

charged glass slides. Tissues were permeabilized as above, blocked with either 10% goat serum or M.O.M blocking serum (Vector Laboratories), and incubated with primary antibody overnight at 4°C, followed by AlexaFluor 488 and/or AlexaFluor 555 secondary antibodies (Molecular Probes). Immunofluorescence was visualized using a Leica TCS SP5 inverted confocal microscope. Quantitative analysis of subnuclear localization was done using ImageJ software (Abramoff et al., 2004).

Fluorescence In Situ Hybridization (FISH)

FISH analysis was done using 5-Carboxyl-X-rhodamine (5-ROX) labeled BAC DNA (Empire Genomics). Cells were trypsinized, treated with 0.38% KCl, fixed in 3:1 methanol-acetic acid, and subjected to FISH hybridization following the procedure recommended by Empire Genomics. Fluorescence signals were captured on Leica TCS SP5 inverted confocal microscope and quantified using ImageJ software. Hybridization signals were scored for at least 100 interphase nuclei for each probe to determine the location of the FISH signal in the nucleus. Experiments were performed three independent times for each probe.

Analyses of Proteins

Immunoprecipitation assays from C2C12 cells or 293T cells were done using total protein extracts obtained by lysis in RIPA buffer (Lee et al., 2004, 2006); immunoprecipitation assays from limb nuclear extracts were done in BC200 containing 0.1% NP40. Samples were incubated with anti-Flag Affinity beads (Sigma-Aldrich) or protein-specific antibodies (as indicated) followed by precipitation with protein A or Protein G beads. Immunoprecipitated proteins were eluted using Flag peptide (Sigma-Aldrich) or by addition of 1× SDS sample buffer and analyzed by immunoblotting using an ECL Plus Western Blotting Detection Kit (GE Healthcare).

Histone Methyltransferase (HMT) Assays

HMT assays were done by incubating Msx1 protein or the immunopurified protein complex with nucleosomes made with recombinant core histone containing wild-type histone H3 or mutated variants of histone H3 plus radiolabeled *S*-Adenosylmethionine as in (Kuzmichev et al., 2004); proteins were resolved by SDS-PAGE and visualized by autoradiography.

Statistical Analyses

At least three independent experiments were performed for each assay. The average values of the parallel experiments are given as the mean ± SD. Comparison of differences among the groups was carried out by two-tailed Student's t test. Significance was defined as $p < 0.01$ (***$p < 0.0001$; **$p < 0.001$; * $p < 0.01$).

Detailed information is provided in Supplemental Experimental Procedures.

ACCESSION NUMBERS

Gene expression microarray data have been deposited in the Gene Expression Omnibus (GEO) under series accession number GSE26021; ChIP-Seq data have been deposited in GEO under series accession number GSE26711.

SUPPLEMENTAL INFORMATION

Supplemental Information includes seven figures, six tables, and Supplemental Experimental Procedures and can be found with this article online at doi:10.1016/j.devcel.2011.07.003.

ACKNOWLEDGMENTS

We are indebted to Drs. Danny Reinberg and Raphael Margueron for providing reagents and many helpful discussions, Dr. Murty Vundavalli for assistance with FISH, and Dr. Manus Biggs for assistance with ImageJ. We are grateful to Dr. Robert Maxson for providing the *Msx1* and *Msx2* conditional mice, Drs. David Sassoon and Virginia E. Papaioannou for plasmids, and Susan Morton and Dr. Thomas M. Jessell for the *Msx* antibody. We thank Lejuan F. Chatman, Celia D. Keim, and Songyan Han for technical assistance, Garrett Frampton, David Orlando, and Stuart Levine for computational support with ChIP-Seq analyses, George Bell and the Whitehead Bioinformatics and Research Computing group for assistance with expression analyses, members of the Young and Abate-Shen laboratories for helpful discussions, and Dr. Michael Shen for helpful discussions and comments on the manuscript. R.M.K. was supported by an American Cancer Society postdoctoral fellowship. This work was supported by The T.J. Martell Foundation for Leukemia, Cancer and AIDS Research (C.A.-S.) and by grants HG002668 (R.A.Y.) and HD029446 (C.A.-S.).

Received: December 24, 2010
Revised: April 15, 2011
Accepted: July 7, 2011
Published online: August 18, 2011

REFERENCES

Abramoff, M.D., Magelhaes, P.J., and Ram, S.J. (2004). Image Processing with ImageJ. Biophotonics Int. *11*, 36–42.

Bendall, A.J., and Abate-Shen, C. (2000). Roles for Msx and Dlx homeoproteins in vertebrate development. Gene *247*, 17–31.

Bendall, A.J., Ding, J., Hu, G., Shen, M.M., and Abate-Shen, C. (1999). Msx1 antagonizes the myogenic activity of Pax3 in migrating limb muscle precursors. Development *126*, 4965–4976.

Boyer, L.A., Plath, K., Zeitlinger, J., Brambrink, T., Medeiros, L.A., Lee, T.I., Levine, S.S., Wernig, M., Tajonar, A., Ray, M.K., et al. (2006). Polycomb complexes repress developmental regulators in murine embryonic stem cells. Nature *441*, 349–353.

Bracken, A.P., Dietrich, N., Pasini, D., Hansen, K.H., and Helin, K. (2006). Genome-wide mapping of Polycomb target genes unravels their roles in cell fate transitions. Genes Dev. *20*, 1123–1136.

Buchberger, A., Freitag, D., and Arnold, H.H. (2007). A homeo-paired domain-binding motif directs Myf5 expression in progenitor cells of limb muscle. Development *134*, 1171–1180.

Cao, R., Wang, L., Wang, H., Xia, L., Erdjument-Bromage, H., Tempst, P., Jones, R.S., and Zhang, Y. (2002). Role of histone H3 lysine 27 methylation in Polycomb-group silencing. Science *298*, 1039–1043.

Caretti, G., Di Padova, M., Micales, B., Lyons, G.E., and Sartorelli, V. (2004). The Polycomb Ezh2 methyltransferase regulates muscle gene expression and skeletal muscle differentiation. Genes Dev. *18*, 2627–2638.

Catron, K.M., Wang, H., Hu, G., Shen, M.M., and Abate-Shen, C. (1996). Comparison of MSX-1 and MSX-2 suggests a molecular basis for functional redundancy. Mech. Dev. *55*, 185–199.

Cornelison, D.D., Olwin, B.B., Rudnicki, M.A., and Wold, B.J. (2000). MyoD(-/-) satellite cells in single-fiber culture are differentiation defective and MRF4 deficient. Dev. Biol. *224*, 122–137.

Davidson, D. (1995). The function and evolution of Msx genes: pointers and paradoxes. Trends Genet. *11*, 405–411.

Davidson, D.R., Crawley, A., Hill, R.E., and Tickle, C. (1991). Position-dependent expression of two related homeobox genes in developing vertebrate limbs. Nature *352*, 429–431.

Ezhkova, E., Pasolli, H.A., Parker, J.S., Stokes, N., Su, I.H., Hannon, G., Tarakhovsky, A., and Fuchs, E. (2009). Ezh2 orchestrates gene expression for the stepwise differentiation of tissue-specific stem cells. Cell *136*, 1122–1135.

Fraser, P., and Bickmore, W. (2007). Nuclear organization of the genome and the potential for gene regulation. Nature *447*, 413–417.

Fu, H., Ishii, M., Gu, Y., and Maxson, R. (2007). Conditional alleles of Msx1 and Msx2. Genesis *45*, 477–481.

Goldhamer, D.J., Brunk, B.P., Faerman, A., King, A., Shani, M., and Emerson, C.P., Jr. (1995). Embryonic activation of the myoD gene is regulated by a highly conserved distal control element. Development *121*, 637–649.

Hadchouel, J., Carvajal, J.J., Daubas, P., Bajard, L., Chang, T., Rocancourt, D., Cox, D., Summerbell, D., Tajbakhsh, S., Rigby, P.W., and Buckingham, M. (2003). Analysis of a key regulatory region upstream of the Myf5 gene

reveals multiple phases of myogenesis, orchestrated at each site by a combination of elements dispersed throughout the locus. Development *130*, 3415–3426.

Houzelstein, D., Auda-Boucher, G., Chéraud, Y., Rouaud, T., Blanc, I., Tajbakhsh, S., Buckingham, M.E., Fontaine-Pérus, J., and Robert, B. (1999). The homeobox gene Msx1 is expressed in a subset of somites, and in muscle progenitor cells migrating into the forelimb. Development *126*, 2689–2701.

Hu, G., Lee, H., Price, S.M., Shen, M.M., and Abate-Shen, C. (2001). Msx homeobox genes inhibit differentiation through upregulation of cyclin D1. Development *128*, 2373–2384.

Kuzmichev, A., Nishioka, K., Erdjument-Bromage, H., Tempst, P., and Reinberg, D. (2002). Histone methyltransferase activity associated with a human multiprotein complex containing the Enhancer of Zeste protein. Genes Dev. *16*, 2893–2905.

Kuzmichev, A., Jenuwein, T., Tempst, P., and Reinberg, D. (2004). Different EZH2-containing complexes target methylation of histone H1 or nucleosomal histone H3. Mol. Cell *14*, 183–193.

Lallemand, Y., Nicola, M.A., Ramos, C., Bach, A., Cloment, C.S., and Robert, B. (2005). Analysis of Msx1; Msx2 double mutants reveals multiple roles for Msx genes in limb development. Development *132*, 3003–3014.

Lanctôt, C., Cheutin, T., Cremer, M., Cavalli, G., and Cremer, T. (2007). Dynamic genome architecture in the nuclear space: regulation of gene expression in three dimensions. Nat. Rev. Genet. *8*, 104–115.

Lee, H., Habas, R., and Abate-Shen, C. (2004). MSX1 cooperates with histone H1b for inhibition of transcription and myogenesis. Science *304*, 1675–1678.

Lee, H., Quinn, J.C., Prasanth, K.V., Swiss, V.A., Economides, K.D., Camacho, M.M., Spector, D.L., and Abate-Shen, C. (2006). PIAS1 confers DNA-binding specificity on the Msx1 homeoprotein. Genes Dev. *20*, 784–794.

Margueron, R., and Reinberg, D. (2010). Chromatin structure and the inheritance of epigenetic information. Nat. Rev. Genet. *11*, 285–296.

Marson, A., Levine, S.S., Cole, M.F., Frampton, G.M., Brambrink, T., Johnstone, S., Guenther, M.G., Johnston, W.K., Wernig, M., Newman, J., et al. (2008). Connecting microRNA genes to the core transcriptional regulatory circuitry of embryonic stem cells. Cell *134*, 521–533.

Mendenhall, E.M., Koche, R.P., Truong, T., Zhou, V.W., Issac, B., Chi, A.S., Ku, M., and Bernstein, B.E. (2010). GC-rich sequence elements recruit PRC2 in mammalian ES cells. PLoS Genet. *6*, e1001244.

Mikkelsen, T.S., Ku, M., Jaffe, D.B., Issac, B., Lieberman, E., Giannoukos, G., Alvarez, P., Brockman, W., Kim, T.K., Koche, R.P., et al. (2007). Genome-wide maps of chromatin state in pluripotent and lineage-committed cells. Nature *448*, 553–560.

Misteli, T. (2007). Beyond the sequence: cellular organization of genome function. Cell *128*, 787–800.

Odelberg, S.J., Kollhoff, A., and Keating, M.T. (2000). Dedifferentiation of mammalian myotubes induced by msx1. Cell *103*, 1099–1109.

Satokata, I., and Maas, R. (1994). Msx1 deficient mice exhibit cleft palate and abnormalities of craniofacial and tooth development. Nat. Genet. *6*, 348–356.

Schuettengruber, B., and Cavalli, G. (2009). Recruitment of polycomb group complexes and their role in the dynamic regulation of cell fate choice. Development *136*, 3531–3542.

Schwartz, Y.B., and Pirrotta, V. (2007). Polycomb silencing mechanisms and the management of genomic programmes. Nat. Rev. Genet. *8*, 9–22.

Seenundun, S., Rampalli, S., Liu, Q.C., Aziz, A., Palii, C., Hong, S., Blais, A., Brand, M., Ge, K., and Dilworth, F.J. (2010). UTX mediates demethylation of H3K27me3 at muscle-specific genes during myogenesis. EMBO J. *29*, 1401–1411.

Sing, A., Pannell, D., Karaiskakis, A., Sturgeon, K., Djabali, M., Ellis, J., Lipshitz, H.D., and Cordes, S.P. (2009). A vertebrate Polycomb response element governs segmentation of the posterior hindbrain. Cell *138*, 885–897.

Towbin, B.D., Meister, P., and Gasser, S.M. (2009). The nuclear envelope—a scaffold for silencing? Curr. Opin. Genet. Dev. *19*, 180–186.

Ventura, A., Kirsch, D.G., McLaughlin, M.E., Tuveson, D.A., Grimm, J., Lintault, L., Newman, J., Reczek, E.E., Weissleder, R., and Jacks, T. (2007). Restoration of p53 function leads to tumour regression in vivo. Nature *445*, 661–665.

Woloshin, P., Song, K., Degnin, C., Killary, A.M., Goldhamer, D.J., Sassoon, D., and Thayer, M.J. (1995). MSX1 inhibits myoD expression in fibroblast x 10T1/2 cell hybrids. Cell *82*, 611–620.

Woo, C.J., Kharchenko, P.V., Daheron, L., Park, P.J., and Kingston, R.E. (2010). A region of the human HOXD cluster that confers polycomb-group responsiveness. Cell *140*, 99–110.

Yao, J., Fetter, R.D., Hu, P., Betzig, E., and Tjian, R. (2011). Subnuclear segregation of genes and core promoter factors in myogenesis. Genes Dev. *25*, 569–580.

Yu, M., Riva, L., Xie, H., Schindler, Y., Moran, T.B., Cheng, Y., Yu, D., Hardison, R., Weiss, M.J., Orkin, S.H., et al. (2009). Insights into GATA-1-mediated gene activation versus repression via genome-wide chromatin occupancy analysis. Mol. Cell *36*, 682–695.

Zhang, H., Catron, K.M., and Abate-Shen, C. (1996). A role for the Msx-1 homeodomain in transcriptional regulation: residues in the N-terminal arm mediate TATA binding protein interaction and transcriptional repression. Proc. Natl. Acad. Sci. USA *93*, 1764–1769.

Zhang, H., Hu, G., Wang, H., Sciavolino, P., Iler, N., Shen, M.M., and Abate-Shen, C. (1997). Heterodimerization of Msx and Dlx homeoproteins results in functional antagonism. Mol. Cell. Biol. *17*, 2920–2932.

Zhao, R., Bodnar, M.S., and Spector, D.L. (2009). Nuclear neighborhoods and gene expression. Curr. Opin. Genet. Dev. *19*, 172–179.